

AD-A155 286 DEVELOPMENT OF ULTRASONIC MODELING TECHNIQUES FOR THE
STUDY OF CRUSTAL IN. (U) MASSACHUSETTS INST OF TECH
CAMBRIDGE DEPT OF EARTH ATMOSPHERI.
UNCLASSIFIED J T BULLITT ET AL. AUG 84 SCIENTIFIC-1 F/G 8/1

DEVELOPMENT OF ULTRASONIC MODELING TECHNIQUES FOR THE
STUDY OF CRUSTAL IN. (U) MASSACHUSETTS INST OF TECH
CAMBRIDGE DEPT OF EARTH ATMOSPHERIC
J T BULLITT ET AL. AUG 84 SCIENTIFIC-1 F/G 8/1

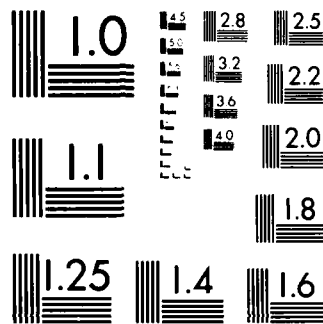
1/1.

UNCLASSIFIED

F/G 8/1

NL

[illegible]



MICROCOPY RESOLUTION TEST CHART
NATIONAL BUREAU OF STANDARDS-1963-A

AFGL-TR-84-0227

DEVELOPMENT OF ULTRASONIC MODELING TECHNIQUES
FOR THE STUDY OF CRUSTAL INHOMOGENEITIES

John T. Bullitt

M. Nafi Toksöz

Earth Resources Laboratory
Department of Earth, Atmospheric, and Planetary Sciences
Massachusetts Institute of Technology
Cambridge, Massachusetts 02139

Scientific Report No. 1

August 1984

Approved for public release; distribution unlimited

AIR FORCE GEOPHYSICS LABORATORY
AIR FORCE SYSTEMS COMMAND
UNITED STATES AIR FORCE
HANSCOM AFB, MASSACHUSETTS 01741

DTIC
ELECTE
JUN 12 1985
G

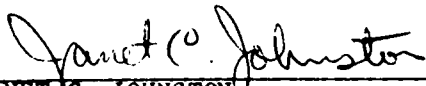
85 5 17 176

AD-A155 206

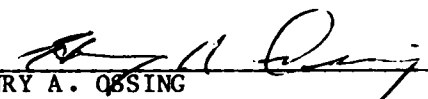
NOT FOR COPY

CONTRACTOR REPORTS

This technical report has been reviewed and is approved for publication.



JANET C. JOHNSTON
Contract Manager



HENRY A. OSSING
Chief, Solid Earth Geophysics Branch

FOR THE COMMANDER



DONALD H. ECKHARDT
Director
Earth Sciences Division

This report has been reviewed by the ESD Public Affairs Office (PA) and is releasable to the National Technical Information Service (NTIS).

Qualified requestors may obtain additional copies from the Defense Technical Information Center. All others should apply to the National Technical Information Service.

If your address has changed, or if you wish to be removed from the mailing list, or if the addressee is no longer employed by your organization, please notify AFGL/DAA, Hanscom AFB, MA 01731. This will assist us in maintaining a current mailing list.

unclassified

SECURITY CLASSIFICATION OF THIS PAGE (When Data Entered)

REPORT DOCUMENTATION PAGE		READ INSTRUCTIONS BEFORE COMPLETING FORM																				
1. REPORT NUMBER AFGL-TR-84-0227	2. GOVT ACCESSION NO.	3. RECIPIENT'S CATALOG NUMBER																				
4. TITLE (and Subtitle) Development of Ultrasonic Modeling Techniques for the Study of Crustal Inhomogeneities		5. TYPE OF REPORT & PERIOD COVERED Scientific Report No. 1																				
7. AUTHOR(s) John T. Bullitt M. Nafi Toksöz		6. PERFORMING ORG. REPORT NUMBER																				
9. PERFORMING ORGANIZATION NAME AND ADDRESS Earth Resources Laboratory, Dept. of Earth, Atmospheric, and Planetary Sciences, M.I.T. Cambridge, MA 02139		8. CONTRACT OR GRANT NUMBER(s) F19628-83-K-0027																				
11. CONTROLLING OFFICE NAME AND ADDRESS Air Force Geophysics Laboratory Hanscom AFB, Massachusetts 01731 Monitor/ Janet C. Johnston/LWH		10. PROGRAM ELEMENT, PROJECT, TASK AREA & WORK UNIT NUMBERS 61102F 2309G2AP																				
14. MONITORING AGENCY NAME & ADDRESS (if different from Controlling Office)		12. REPORT DATE August 1984																				
		13. NUMBER OF PAGES 35																				
		15. SECURITY CLASS. (of this report) unclassified																				
		15a. DECLASSIFICATION/DOWNGRADING SCHEDULE																				
16. DISTRIBUTION STATEMENT (of this Report) Approved for public release; distribution unlimited																						
17. DISTRIBUTION STATEMENT (of the abstract entered in Block 20, if different from Report)		<table border="1"> <tr> <td colspan="2">Accession For</td> </tr> <tr> <td>NTIS GRA&I</td> <td><input checked="" type="checkbox"/></td> </tr> <tr> <td>DTIC TAB</td> <td><input type="checkbox"/></td> </tr> <tr> <td>Unannounced</td> <td><input type="checkbox"/></td> </tr> <tr> <td>Justification</td> <td></td> </tr> <tr> <td colspan="2">By _____</td> </tr> <tr> <td colspan="2">Distribution/</td> </tr> <tr> <td colspan="2">Availability Codes</td> </tr> <tr> <td>Dist</td> <td>Avail and/or Special</td> </tr> <tr> <td>A/</td> <td></td> </tr> </table>	Accession For		NTIS GRA&I	<input checked="" type="checkbox"/>	DTIC TAB	<input type="checkbox"/>	Unannounced	<input type="checkbox"/>	Justification		By _____		Distribution/		Availability Codes		Dist	Avail and/or Special	A/	
Accession For																						
NTIS GRA&I	<input checked="" type="checkbox"/>																					
DTIC TAB	<input type="checkbox"/>																					
Unannounced	<input type="checkbox"/>																					
Justification																						
By _____																						
Distribution/																						
Availability Codes																						
Dist	Avail and/or Special																					
A/																						
18. SUPPLEMENTARY NOTES																						
19. KEY WORDS (Continue on reverse side if necessary and identify by block number) ultrasonic modeling, scattering, crustal inhomogeneities																						
20. ABSTRACT (Continue on reverse side if necessary and identify by block number) The effects of topographic features on Rayleigh wave propagation and scattering are investigated in the laboratory using three-dimensional ultrasonic models. Starting from simple steps, different topographic features are modeled. The effects of these features on Rayleigh wave transmission and scattering are examined as a function of wavelength and as a function of angle of incidence. In general, back scattered or reflected Rayleigh waves are small compared to transmitted waves. A significant fraction of the Rayleigh wave energy is scattered into body waves. Transmission and reflection coefficients (transmitted																						

DD FORM 1 JAN 73 1473

EDITION OF 1 NOV 65 IS OBSOLETE

unclassified

SECURITY CLASSIFICATION OF THIS PAGE (When Data Entered)

(20 cont'd.)

or reflected energy/incident energy) computed from spectra ratios vary strongly with incidence angle. At wavelengths equal to twice the step height, the fraction of incident energy scattered into body waves ranges from more than 90% at normal incidence to about zero at near-grazing incidence. At each angle, transmission coefficients vary strongly with frequency. Because of frequency-dependent phase shifts, the transmitted and reflected waves are distorted.

The effect of the steps on the propagation of Rayleigh waves is demonstrated by convolving synthetic dispersed wave trains with the impulse response of the scale models. The ocean-continent margin of the western United States is modeled as a 60° ramp scaled to 60 km height. The Tibetan Plateau is modeled as a broad mesa scaled to 40 km height. In both models the azimuthal dependence of transmitted Rayleigh waves is similar to that observed at WWSSN stations for Rayleigh waves crossing the modeled terrestrial structures.

ABSTRACT

The effects of topographic features on Rayleigh wave propagation and scattering are investigated in the laboratory using three-dimensional ultrasonic models. Starting from simple steps, different topographic features are modeled. The effects of these features on Rayleigh wave transmission and scattering are examined as a function of wavelength and as a function of angle of incidence. In general, backscattered or reflected Rayleigh waves are small compared to transmitted waves. A significant fraction of the Rayleigh wave energy is scattered into body waves. Transmission and reflection coefficients (transmitted or reflected energy/incident energy) computed from spectral ratios vary strongly with incidence angle. At wavelengths equal to twice the step height, the fraction of incident energy scattered into body waves ranges from more than 90% at normal incidence to about zero at near-grazing incidence. At each angle, transmission coefficients vary strongly with frequency. Because of frequency-dependent phase shifts, the transmitted and reflected waves are distorted.

The effect of the steps on the propagation of Rayleigh waves is demonstrated by convolving synthetic dispersed wave trains with the impulse response of the scale models. This is done using the transmission response function at the appropriate angle and from the simple model described above and convolving with the input wave function. The ocean-continent margin of the western United States is modeled as a 60° ramp scaled to 60 km height. The Tibetan Plateau is modeled as a broad mesa scaled to 40 km height. In both models the azimuthal dependence of transmitted Rayleigh waves is similar to that observed at WSSN stations for Rayleigh waves crossing the modeled terrestrial structures. The actual physical modelling of the plateaus is now underway using simple shapes (such as circular mesas) at first.

INTRODUCTION

Rayleigh wave propagation in strongly-varying structures is a complex process well suited to analysis by ultrasonic modeling methods. Until recently, ultrasonic modeling of surface wave transmission and scattering has been limited to two dimensions. In this paper we report on a series of ultrasonic modeling experiments investigating the propagation and scattering of Rayleigh waves by simple three-dimensional topographic features.

Rayleigh waves propagating in two dimensions through simple steps or around corners and in wedges have been studied experimentally by a number of investigators (de Bremaecker, 1958; Kato and Takagi, 1956; Lewis and Dally, 1970; Knopoff and Gangi, 1960; Pilant *et al.*, 1964; Martell *et al.*, 1977; and Nathman, 1980). Detailed 'snapshots' of the complete stress field of Rayleigh waves scattered in wedges have been obtained using photoelastic methods (Lewis and Dally, 1970).

Development of theoretical and numerical methods of synthesizing Rayleigh waves scattered from simple structures has typically lagged behind experimental results. Rayleigh wave transmission and reflection coefficients across vertical boundaries in two dimensions have been calculated using approximate variational methods (e.g. McGarr and Alsop, 1967). Recently, synthesis of complete seismograms of Rayleigh waves reflected from, and transmitted through, a vertical step has been performed using the finite-difference method (Toksöz 1983; Fuyuki and Nakano, 1984). In three dimensions, numerical computations are limited

Approximate methods to estimate transmission and reflection coefficients of Rayleigh waves incident at steep angles on a vertical boundary have, however, been developed (Malichewsky, 1976; Chen and Alsop, 1979).

Scattering of Rayleigh waves in three dimensions can be investigated in the laboratory using ultrasonic methods. Rayleigh wave propagation in three-dimensions has been studied using realistic three-dimensional scale models of surface topography (e.g. Toksöz, 1983). In such models even a simple input pulse is severely distorted by the complex structure. Subtle effects of topography on Rayleigh wave propagation and scattering are thus easily obscured by the complexity of the model. An important step toward an understanding of surface wave scattering in three-dimensions is the investigation of propagation in simple models of canonical form.

In this paper, we investigate Rayleigh wave scattering from step and ramp-type topographic discontinuities and study their implications for surface wave propagation across major features such as ocean-continent boundaries and Tibet.

EXPERIMENTAL METHOD

The model used in this study consists of a solid block ($200 \times 200 \times 100 \text{ mm}^3$) of aluminum. Steps of various height and geometry are milled into one of the large faces (Figure 1).

The ultrasonic source and receiver each consist of a 2.25 MHz P wave transducer coupled to a lucite wedge. The geometry of the wedges is such that P waves generated by the transducer excite Rayleigh waves in the aluminum with high efficiency. Similarly, the transducer is an efficient Rayleigh wave sensor. The radiation pattern of the transducer-wedge combination is highly directional; at an angle of 10° from the axis of the central lobe, peak energy is reduced to less than 25% the axial peak energy. The combination of these features makes the transducer-wedge combination especially useful when working with a low-loss medium such as aluminum; attenuation can be neglected in the analysis of Rayleigh wave propagation, and the observed Rayleigh waves are uncontaminated by body waves multiply reflected at the edges of the model.

Peak energy of Rayleigh waves traveling on the aluminum block ($V_p = 6.4 \text{ km/sec}$; $V_s = 3.2 \text{ km/sec}$; $c_R = 3.0 \text{ km/sec}$) lies in the range 0.2–2.0 MHz ($\lambda = 1.5\text{--}15 \text{ mm}$). In this frequency band the spectrum is repeatably obtained from a given model and source-receiver configuration. We therefore take this as the usable bandwidth of the modeling experiments. Because the model is essentially a half-space, only fundamental-mode Rayleigh waves are observed. Since a half-space is non-dispersive to Rayleigh waves, the half-space Rayleigh wave represents the impulse response of the transducers and recording system.

When a Rayleigh wave encounters a step some of the incident energy is transmitted through the step, some is reflected from the step, and some is converted to body waves (de Bremaecker, 1958; Knopoff and Gangi, 1960; Martel *et al.*, 1977; Toksöz, 1983). In general the efficiency of transmission through or

reflection from a step depends on the wavelength relative to the step height (e.g. McGarr and Alsop, 1967). In order to facilitate comparison of models with different step heights, therefore, wavelengths are normalized to the step height. The "normalized frequency", \hat{f} , is obtained from the scaling relation

$$\hat{f} = \frac{hf}{c} = \frac{h}{\lambda} \quad (1)$$

where f is the frequency, c is the phase velocity, λ is the wavelength, and h is the step height. For a given step height, the range of usable normalized frequencies is limited by the usable bandwidth of the modeling experiments. This is an important consideration when the model seismograms are scaled to correspond to real Earth seismograms. Transmission and reflection coefficients calculated from Rayleigh waves traveling across steps of various heights indicate that the model scaling relation (Equation 1) is generally appropriate over a wide range of frequencies and step heights.

We define the the Rayleigh wave energy transmission coefficient, E_T , as

$$E_T(\hat{f}) = \left[\frac{A_T(\hat{f})}{A_0(\hat{f})} \right]^2, \quad (2a)$$

where $A_T(\hat{f})$ is the Fourier amplitude spectrum of the transmitted Rayleigh wave, and $A_0(\hat{f})$ is the amplitude spectrum of the Rayleigh wave propagating across the aluminum half-space. The reflection coefficient, E_R , is defined in an exactly analogous way:

$$E_R(\hat{f}) = \left[\frac{A_R(\hat{f})}{A_0(\hat{f})} \right]^2, \quad (2b)$$

where $A_R(\hat{f})$ is the amplitude spectrum of the reflected Rayleigh wave.

Transmitted Rayleigh waves are recorded by keeping source and receiver at opposite points on the diameter of a circle centered on the step (see Figure 1). Reflected waves are observed by placing source and receiver at equal angles from the normal to the strike of the step. Incidence angle is measured from the

strike of the step.

MODELING RESULTS

VERTICAL STEP MODEL

Figure 2 shows seismograms of Rayleigh waves transmitted across a 3mm vertical step at incidence angles ranging from 15° through 90° (normal incidence). The small signal arriving about $1 \mu\text{sec}$ before the Rayleigh wave is an S wave excited at the step. At a given incidence angle the waveforms for the case of up- and down-step transmission are essentially identical. Note that not only peak amplitudes decrease by a factor of two to four or more, but also the waveform changes strongly as a function of angle of incidence. At normal incidence ($\theta=90^\circ$) transmission coefficients (Figure 3) agree well with those obtained for a two-dimensional step using theoretical (numerical) calculations (Drake, 1972; Martel *et al.*, 1977; Fuyuki and Nakano, 1984).

At normal incidence the fraction of transmitted energy (E_T) seldom exceeds 20% within the usable frequency band. This represents a loss of over 80% of the incident Rayleigh wave energy to reflected surface waves and converted body waves.

Reflected Rayleigh wave seismograms are complicated by the presence of double reflections, separated by about $2 \mu\text{sec}$ (Figure 4). In Figure 4A, the first reflection corresponds to the Rayleigh wave reflected from the bottom edge of the step; the second to the Rayleigh wave reflected from the upper edge after propagating up the face of the step. These are further complicated by multiple scattering and Rayleigh to shear scattering. Reflections from a down-step (Figure 4B) are much larger than those from an up-step (Figure 4A). Also, shapes of down-step reflected waveforms are different from those of up-step. They do not exhibit the strong incidence angle dependence. Similar differences in up-step, down-step scattering of Rayleigh waves have been observed in two-dimensional

modeling experiments (e.g. Nathman, 1980).

In general the reflected energy is very small, particularly at normal or near-normal incidence (Figure 6). At most angles and frequencies, reflected energy accounts for no more than 10-20% of the incident energy. As the incidence angle becomes more grazing the reflected energy increases rapidly, especially for wavelengths approximately equal to three times the step height ($\hat{f} \approx 0.3$).

It is clear from Figures 3 and 5 that the efficiency of body wave scattering is strongly dependent on the angle of incidence. In the 3 mm step model, at wavelengths equal to one-half the step height (the first maximum in Figure 3) about 90% of the incident energy is scattered to body waves. As the incidence angle θ increases to near 0° (grazing incidence), this figure drops to about zero.

RAISED MODEL

To investigate the effect of a more gradual change of elevation, the 3mm step was tapered to a slope of 60° from the horizontal (see Figure 1). Distortion of both transmitted and reflected waveforms is strong, particularly at normal and near normal incidence (Figure 6).

Energy transmission coefficients for this model (Figure 7a) are generally lower than those for the step model (Figure 3b) at frequencies below $\hat{f} \approx 0.5$. The energy minimum near $\hat{f} \approx 0.9$ at normal incidence is considerably smaller than the corresponding minimum for the step model. Reflected energy (Figure 7b) is considerably smaller than for the case of the vertical step (Figure 4a). The double reflection is, however, apparent at all angles. Interference between the two reflections and the scattered body waves contribute to the complexity of the seismograms.

INPUT

$\theta = 90^\circ$

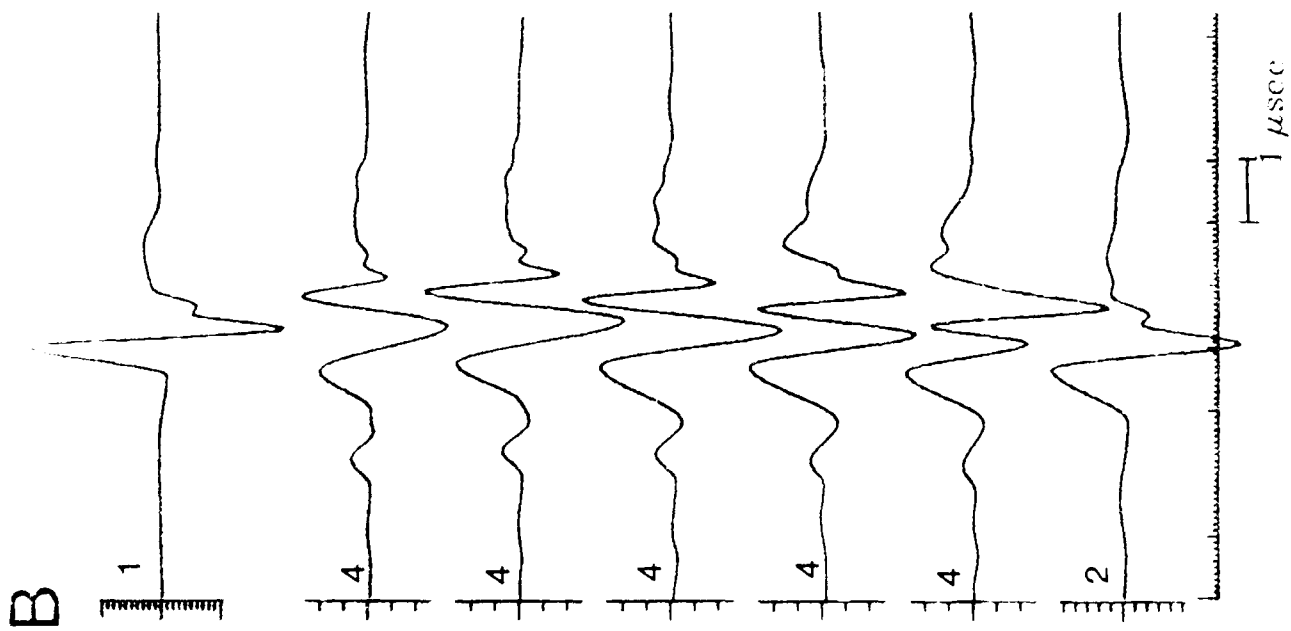
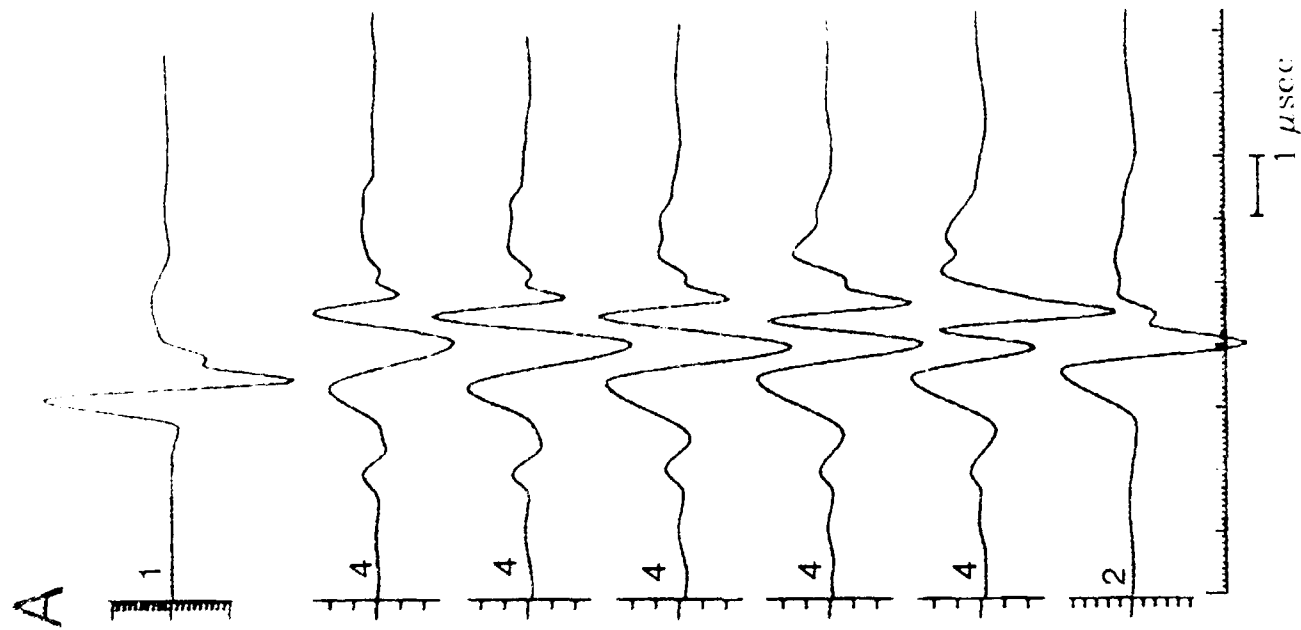
$\theta = 75^\circ$

$\theta = 60^\circ$

$\theta = 45^\circ$

$\theta = 30^\circ$

$\theta = 15^\circ$



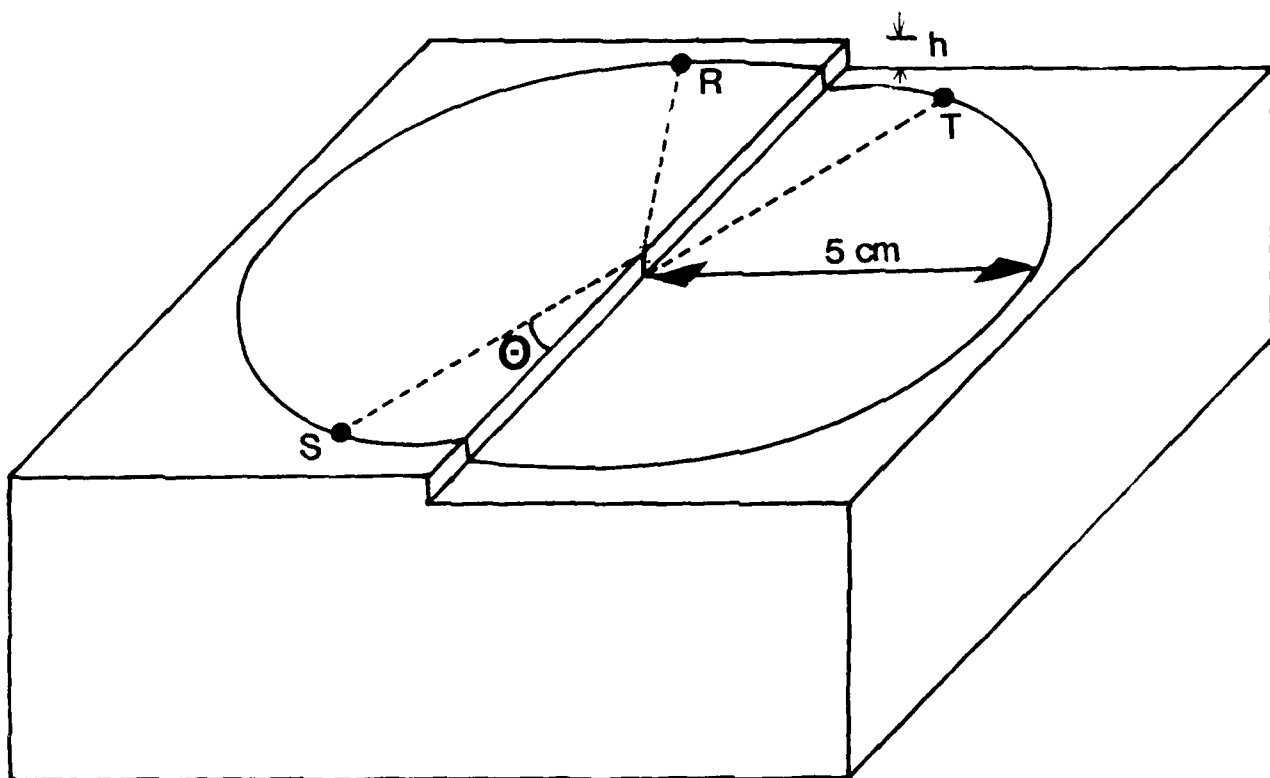


Figure 1

Figure 10. The region in h - λ space in which the ultrasonic model results from the 3mm models may be reliably used. Units of h and λ are arbitrary. In the shaded areas repeatability and consistency of a given experiment is not assured. The usable and unusable regions are demarcated by the maximum and minimum usable normalized frequencies. The box shows the region allowed for modeling Rayleigh waves in the period range 15-40 sec (50-150 km wavelength). Thus step heights in the range 30-100 km may be modeled successfully over this period range.

Figure 11. **A.** WWSSN vertical component recordings of the Rayleigh waves from an earthquake in the Loyalty Islands (9/6/81, $11^{\circ}02'40.8''$ S, 21.488° S, 169.600° E, depth=31 km, $m_b=5.9$, $M_s=6.2$). The angle at which the great-circle crosses the continental margin is shown next to the continental stations. **B.** Model synthetic seismograms using the 3mm, 60° ramp scaled to 60 km height.

Figure 12. Rayleigh wave paths across the Tibetan Plateau from an explosion at the Lop Nor test site (14 October, 1970). Reproduced from Bird (1976). **Inset:** Three-dimensional model of the Tibetan Plateau used to generate model-synthetic seismograms for the paths Lop Nor-NDI and Lop Nor-SHL.

Figure 13. Comparison of real seismograms (solid lines) with model-synthetic seismograms (dashed lines) using the lens model of Figure 12. All seismograms have been low-pass filtered at 10 second period.

FIGURE CAPTIONS

Figure 1. Geometry of the models used in this study. Source transducer is located at point **S**. Reflected or transmitted waves are recorded at points **R** or **T**. Cross sections of two steps used are shown below.

Figure 2. Waveforms of Rayleigh waves transmitted across a 3mm vertical step. The top trace is the input signal. The small pulse arriving 1.0 μ sec before the Rayleigh wave is an S wave excited at the step. The vertical scales on the seismograms have been expanded by the scaling factors shown at the start of each trace. **A**: Transmission in the up-step direction. **B**: Transmission in the down-step direction.

Figure 3. Energy transmission coefficients for the Rayleigh waves in Figure 2. The horizontal axis is normalized frequency ($\hat{f} = \frac{h}{\lambda}$), where h is the step height and λ is the wavelength. Curves are shown for three angles of incidence. **A**: Transmission in the up-step direction. **B**: Transmission in the down-step direction.

Figure 4. Waveforms of Rayleigh waves reflected from the 3mm vertical step. Note the secondary reflection corresponding to a reflection from the *upper* edge of the step. **A**: Reflection from the up-step. **B**: Reflection from the down-step.

Figure 5. Energy reflection coefficients for the reflected Rayleigh waves in Figure 4. Note the change of vertical scale from Figure 3. **A**: Reflection from the up-step. **B**: Reflection from the down-step.

Figure 6. Seismograms of Rayleigh waves transmitted across **(A)** and reflected from **(B)** the 3mm, 60° ramp. Propagation is in the up-step direction. The seismograms in **(B)** were high-pass filtered at 0.3 MHz at the time of recording to enhance the signal-to-noise ratio.

Figure 7. Energy transmission and reflection coefficients for the Rayleigh waves in Figure 6. **A**: Up-step transmission. **B**: Up-step reflection. Note the difference in the amplitude scales.

Figure 8. Energy transmission data of Figure 3a after application of the empirical relation of Equation (3). The transmission curves for the different incidence angles now coincide.

Figure 9. The effect of the 3mm vertical step **(A)** and ramp **(B)** models on a dispersed wave train. The input signal (top trace) is a linear chirped sinusoid, whose frequency increases from 0.2 to 2.0 MHz in 60 μ sec. The corresponding range of the ratio of step height/wavelength (\hat{f}) is 0.2 to 2.

the step-shaped structure and on the cliff, *Sci. Rep. Tohoku Univ., ser. 5*: 8, pp. 74-86.

Knopoff, L. and A. Gangi (1960), Transmission and reflection of Rayleigh waves by wedges, *Geophysics*, *25*, pp. 1203-1214.

Lewis, D. and J.W. Dally (1970), Photoelastic analysis of Rayleigh wave propagation in wedges, *Geophysics*, *75*: 17, pp. 3387-3398.

Malichewsky, P. (1976), Surface waves in media having lateral heterogeneities, *Pure and Appl. Geophys.*, *114*, pp. 833-843.

Martel, L., M. Munasinghe, and G.W. Farnell, (1977) Transmission and reflection of Rayleigh waves through a step, *Bull. Seis. Soc. Am.*, *67*: 5, pp. 1277-1290.

McGarr, A. and L.E. Alsop (1967), Transmission and reflection of Rayleigh waves at vertical boundaries, *J. Geophys. Res.*, *72*: 8, pp. 2169-2180.

Nathman, D.L. (1980), Rayleigh wave scattering across step discontinuities, M.S. Thesis, Mass. Institute of Technology.

Toksöz, M.N. (1983), Development of ultrasonic modeling technique for the study of crustal inhomogeneities, Final Report to Air Force Geophysics Laboratory, AFGL-TR-83-0070, ADA134501.

White, J.E., *Seismic waves: radiation, transmission, and attenuation*, (New York: 1965, McGraw Hill).

REFERENCES

- Bird, G.P. (1976), Thermal and mechanical evolution of continental convergence zones: Zagros and Himalayas, *Ph.D. thesis*, Massachusetts Institute of Technology, Cambridge, Massachusetts.
- Bird, P. and M.N. Toksöz, Strong attenuation of Rayleigh waves in Tibet, *Nature*, **266**, pp. 161-163.
- de Bremaecker, J. Cl. (1958), Transmission and reflection of Rayleigh waves by corners, *Geophysics*, **23**: 2, pp. 253-266.
- Capon, J. (1970), Analysis of Rayleigh-wave multipath propagation at IASA, *Bull. Seis. Soc. Am.*, **60**: pp. 1701-1731.
- Capon, J. (1971), Comparison of Love- and Rayleigh-wave multipath propagation at IASA, *Bull. Seis. Soc. Am.*, **61**: 5, pp. 1327-1344.
- Chen, T.C. and L.E. Alsop (1979), Reflection and transmission of obliquely incident Rayleigh waves at a vertical discontinuity between two welded quarter-spaces, *Bull. Seis. Soc. Am.*, **69**: 5, pp. 1409-1423.
- Drake, L.A. (1972), Love and Rayleigh waves in nonhorizontally layered media, *Bull. Seis. Soc. Am.*, **62**: 5, pp. 1241-1258.
- Drake, L.A. and B.A. Bolt (1980), Love waves normally incident at a continental boundary, *Bull. Seis. Soc. Am.*, **70**: 4, pp. 1103-1123.
- Dziwonski, A.M., A.L. Hales, and E.R. Lapwood (1975), Parametrically simple Earth models consistent with geophysical data, *J. Phys. Earth Plan. Int.*, **10**: 12-48.
- Evernden, J.F. (1953), Direction of approach of Rayleigh waves and related problems, Part I, *Bull. Seis. Soc. Am.*, **43** pp. 335-374.
- Evernden, J.F. (1954), Direction of approach of Rayleigh waves and related problems, Part II, *Bull. Seis. Soc. Am.*, **44** pp. 159-184.
- Fuyuki, M. and M. Nakano (1984), Finite difference analysis of Rayleigh wave transmission past an upward step change, *Bull. Seis. Soc. Am.*, **74**: 3, pp. 893-911.
- Kato, Y. and A. Takegi (1956), Model seismology (part 3): wave propagation in

which surface waves cross regions of strong structural contrast. In basin-and-range provinces, for example, where crustal Rayleigh waves traverse numerous steps, strong effects can be expected due to compounding of the effects suffered by passage through a single step.

The ultrasonic model-synthetic method may prove useful in more general problems of three-dimensional surface wave scattering, particularly in situations for which analytic or numerical solutions are difficult to obtain.

model-synthetic data.

The agreement between real and modeled waveforms is generally good, particularly at longer periods (Figure 13). Note that the relative amplitudes between SHL and NDI are similar for both the observed and model-synthetic seismograms. No attempt has been made here to model the small-scale scattering in Tibet and the Himalayas; the short period (<15-20 sec) components of the waveforms therefore do not match as well.

CONCLUSIONS

Using three-dimensional ultrasonic modeling techniques, transmission and reflection coefficients as a function of wavelength and incidence angle are obtained for Rayleigh waves propagating in simple step models. The efficiency of Rayleigh wave transmission and reflection varies strongly with both incidence angle and wavelength. At some incidence angles and frequencies as much as 90% of the incident Rayleigh wave energy is scattered into body waves. Transmission coefficients obtained at normal (90°) incidence agree with those obtained with two dimensional modeling methods and two-dimensional finite-difference methods. An empirical relation between transmission coefficients at different incidence angles is obtained for the case of a vertical step. This relation may be applied to two-dimensional theoretical (numerical) calculations of propagation in more complicated structures to obtain estimates of Rayleigh wave transmission coefficients at oblique incidence angles.

The effect of simple structures on Rayleigh wave propagation in the Earth is demonstrated by convolving the impulse response of the models with real or synthetic dispersed wave trains. Some observed features of Rayleigh waves crossing an ocean-continent margin and the Tibetan Plateau are similar to those predicted from model results. The method may be applied to studies in

angle governed by Snell's law (e.g. Evernden, 1953; Capon, 1970). Using the coast and ocean models given by Drake and Bolt (1980) we find that, in the period range of interest in this example (15-40 sec), Rayleigh waves incident on the coast at incidence angles greater than 30° are refracted laterally by no more than about 6° . This is within the uncertainty ($\pm 10^\circ$) in the estimate of incidence angle and so is not an important consideration in this example.

THE TIBETAN PLATEAU

The Tibetan Plateau is often regarded as an isostatically-compensated block of uplifted crustal rock with an average elevation of 5 km (e.g. Bird and Toksöz, 1977). According to the ultrasonic modeling results, we expect that Rayleigh waves crossing the margins of such a block will be scattered at the edges of the block and the waveforms distorted. To investigate the effect of the Tibetan Plateau on Rayleigh waves propagating across it we compare real and model-synthetic Rayleigh wave seismograms for the propagation paths shown in Figure 12.

The Tibetan Plateau is modeled here as a cylindrical lens with effective height of 40km above average terrain (Figure 12, inset). The lens itself lies on a half-space. The lens includes the effects of both the elevated topography of the Tibetan Plateau and the deep crustal root of the Himalayas. Model-synthetic Rayleigh seismograms are generated by convolving an input waveform with the impulse response of the step model appropriate for each of the two edges of the lens. Because the Tibetan Plateau is wide compared to a Rayleigh wavelength, interference arising from multiple reflections from opposite edges of the Plateau is neglected. Since there are no WWSSN stations on the northern front of the Plateau, we use the Rayleigh wave recorded at KBL as an input signal to the lens model. The regional attenuation model of Bird (1976) is applied to the

THE OCEAN-CONTINENT MARGIN

The incidence angle dependence of Rayleigh wave transmission across the ocean-continent margin can be seen in recordings of teleseismic oceanic Rayleigh waves made at coastal stations. For example, Figure 11 shows Rayleigh waves recorded at WSSN stations on the west coast of the United States from an earthquake in the Loyalty Islands. The incidence angle is taken to be the angle between the great-circle path and the continental shelf. For paths to BKS, COR and LON, the angles are 90° , 60° , and 45° , respectively. Among the continental stations in this example, epicentral distance ranges from 87.2° (BKS) to 91.9° (LON). Great-circle azimuths vary by no more than about 1° and source radiation patterns would have the same effect at these stations. Differences between the seismograms recorded at the continental stations are therefore primarily due to variations in the incidence angle. At normal incidence (BKS) most of the Rayleigh wave energy is confined to the first dozen or so cycles, after which time the amplitude decays rapidly to a small value. As the incidence angle decreases to near-grazing, the initial 'packet' of energy broadens and the rate of amplitude decay decreases. This trend is consistent with that observed in the chirped sine synthetics (Figure 9).

Synthetic Rayleigh wave seismograms were generated for a pure oceanic path using the PEM-O model (Dziewonski *et al.*, 1975) and convolved with the impulse response of the 3mm ramp models, scaled to a height of 60 km (Figure 11b). The model-synthetic seismograms exhibit azimuthal behavior similar to that of the real seismograms (Figure 11a).

In this example we have assumed the Rayleigh waves propagate on the great circle path between source and receiver. In fact, the velocity contrast across the ocean-continent margin in the Earth is such that Rayleigh waves of a given period traversing the margin will deviate from the great-circle path by an

$$k = \left(\frac{L_m}{L_e} \right) \left(\frac{V_e}{V_m} \right),$$

and T_X , L_X , and V_X are characteristic times, lengths, and velocities, respectively in either the model (m) or the Earth (e).

In general, the terrestrial scale length appropriate for a given physical problem is considerably greater than that which would be indicated by surface topography alone. In discussions of terrestrial scaling, the terrestrial scale length is not to be interpreted literally as the dimension of any real structure; it is simply the characteristic dimension of a highly simplified model. The topographic expression of the physical model includes the combined effects of terrestrial topography and deep structure. The ultrasonic step models described in the first section of this paper represent a very simplified approximation to complex boundaries of vertical heterogeneities of the earth structure. It is still worthwhile, however, to investigate whether models produce effects similar to those observed in the earth.

We take as the input signal for a given model a real or synthetic terrestrial seismogram. The seismogram is resampled at a rate determined by the model scaling factor, and convolved with the impulse of the model. The result of the convolution is resampled to restore the seismogram to its original (terrestrial) time scale.

Because the usable frequency of Rayleigh waves in the modeling experiments is limited to the band 0.2–2.0 MHz, the range of normalized frequencies available for scale modeling is also limited. The range of step heights and wavelengths which may be modeled reliably given the band-limited nature of the ultrasonic pulse is shown in Figure 10.

impulse response of a given model for waves propagating in a given direction is thus the result of deconvolving the transducer/recording system impulse response from the recorded signal. In the frequency domain we may write

$$\hat{T}_m(\theta; \omega) = \frac{\hat{S}_m(\theta; \omega)}{\hat{S}_{hs}(\omega)} \quad (4)$$

where $\hat{T}_m(\theta; \omega)$ is the complex transfer function for the desired model at incidence angle θ , $\hat{S}_m(\theta; \omega)$ is the complex Fourier spectrum of a Rayleigh wave propagating across the model at angle θ , $\hat{S}_{hs}(\omega)$ is the half-space Rayleigh wave spectrum, and ω is the angular frequency. The inverse Fourier transform of this quantity yields the impulse response of the given model.

As a test of the effect of a step on a dispersed wave train, a chirped sinusoid was convolved with the impulse response of the 3mm vertical step and ramp models at several incidence angles (Figure 9). At some incidence angles and frequencies the envelope of the wave train drops to near zero, suggestive of the "beating" phenomenon frequently observed in seismograms of Rayleigh waves propagating across ocean basins. This beating is usually attributed to multipathing due to lateral heterogeneities along the propagation path (Evernden 1953, 1954). At least part of the amplitude modulation of dispersed Rayleigh wave trains observed in the Earth may be due to propagation across sharp structural features such as those modeled here.

In order to investigate the effect of simple steps on Rayleigh wave propagation in the Earth, the physical dimensions of the model are scaled to correspond with those of some realistic Earth structure. The scaling factor relating the physical dimensions of the Earth to those of the model is given by the linear relation (White, 1965):

$$T_m = k T_e \quad (5)$$

where the scaling factor k is given by

using the empirical relation

$$\hat{f}_{\min}(\Theta) = \frac{\hat{f}_{\min}(90^\circ)}{\sin \Theta}, \quad (3a)$$

where $\hat{f}_{\min}(\Theta)$ is the value of \hat{f} at which the first minimum in the transmission curve appears. When this relation is applied to the entire transmission curve the curves at each incidence angle can be made to coincide (Figure 8). In terms of the effective step height at angle Θ , Equation (2a) implies

$$h_{eff}(\Theta) = h \sin \Theta \quad (3b)$$

To a first approximation the transmission coefficient for an arbitrary incidence angle can thus be estimated from the normal incidence transmission coefficient using this empirical relation. This approximation is poor, however, at incidence angles shallower than about 30°.

Because of its strong incidence angle dependence, the reflection coefficient for the step is difficult to model with a simple empirical relation.

IMPLICATIONS FOR THE EARTH

One of the most interesting features of the ultrasonic results is that both transmitted and reflected Rayleigh wave pulse shapes are severely altered as a result of interaction with the various steps. The waveform distortion is due to the combined effects of frequency-dependent energy transmission and reflection and interference of waves multiply reflected within the step. More complicated input signals, such as dispersed wave trains, can be expected to undergo similar kinds of angle-dependent waveform distortion after propagating across a step.

The effect of a given model on a surface wave signal is determined by convolving the desired input signal with the impulse response of the model. As noted earlier, the Rayleigh wave propagating across the aluminum half-space represents the impulse response of the transducers and recording system. The

Note that in the case of the ramp model the frequencies have been normalized to a step height of $h=3.0$ mm; in fact this normalization is arbitrary. While the vertical change in elevation is indeed 3.0 mm, the distance from the lower edge to the upper edge as measured along the ramp surface is actually larger than this ($\frac{h}{\sin\alpha}$, where α is the ramp angle). This distance may also enter into the scaling relations. Direct comparisons between step and ramp transmission and reflection coefficients may not, therefore, be appropriate when scaled to the same step height.

AZIMUTHAL DEPENDENCE OF SCALING

In the models discussed above, the character of the transmitted and reflected waveforms changes most rapidly as the incidence angle decreases below about 30° . It is in the range 0° to 30° that the behavior of Rayleigh wave propagation departs most strikingly from that predicted by two-dimensional theoretical and approximate methods. At incidence angles greater than 30° simple empirical relations can be found between the results obtained at normal and oblique incidence.

In the case of transmission through the vertical step (Figure 3), note that the energy transmission minimum near $\hat{f}=0.5$ at normal incidence moves to higher frequency as the incidence angle decreases. The equivalent effect is observed for normally incident waves when the step height is decreased. This suggests that the effective step height is dependent on incidence angle. That is, as the incidence angle decreases the incident Rayleigh wave "sees" a shorter step. The functional dependence of effective step height on incidence angle is estimated by finding a simple functional relation between incidence angle and a particular feature in the transmission curves. The normalized frequency at which the first minimum occurs in the transmission curves is approximated well

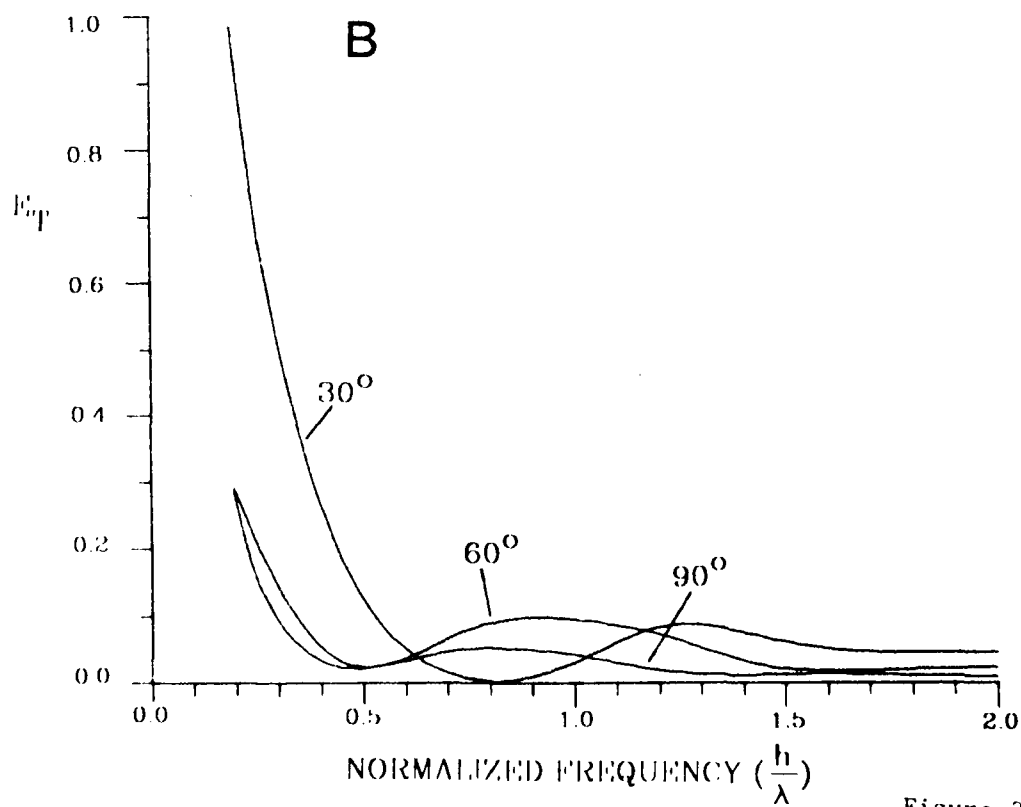
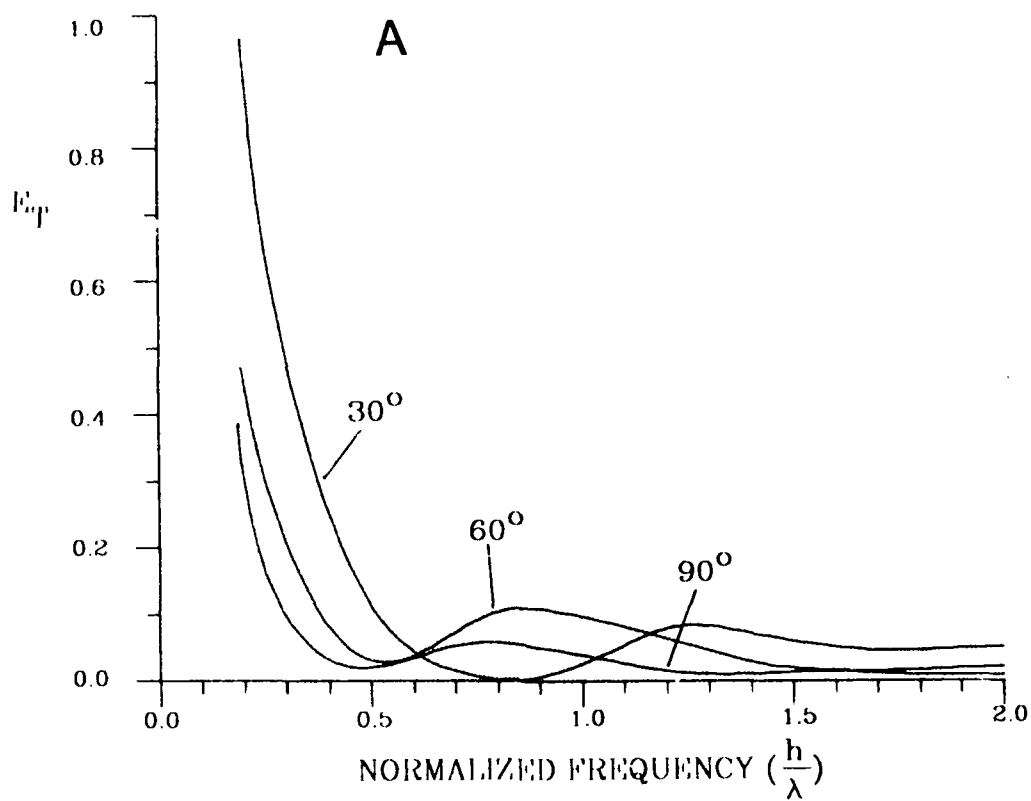


Figure 3

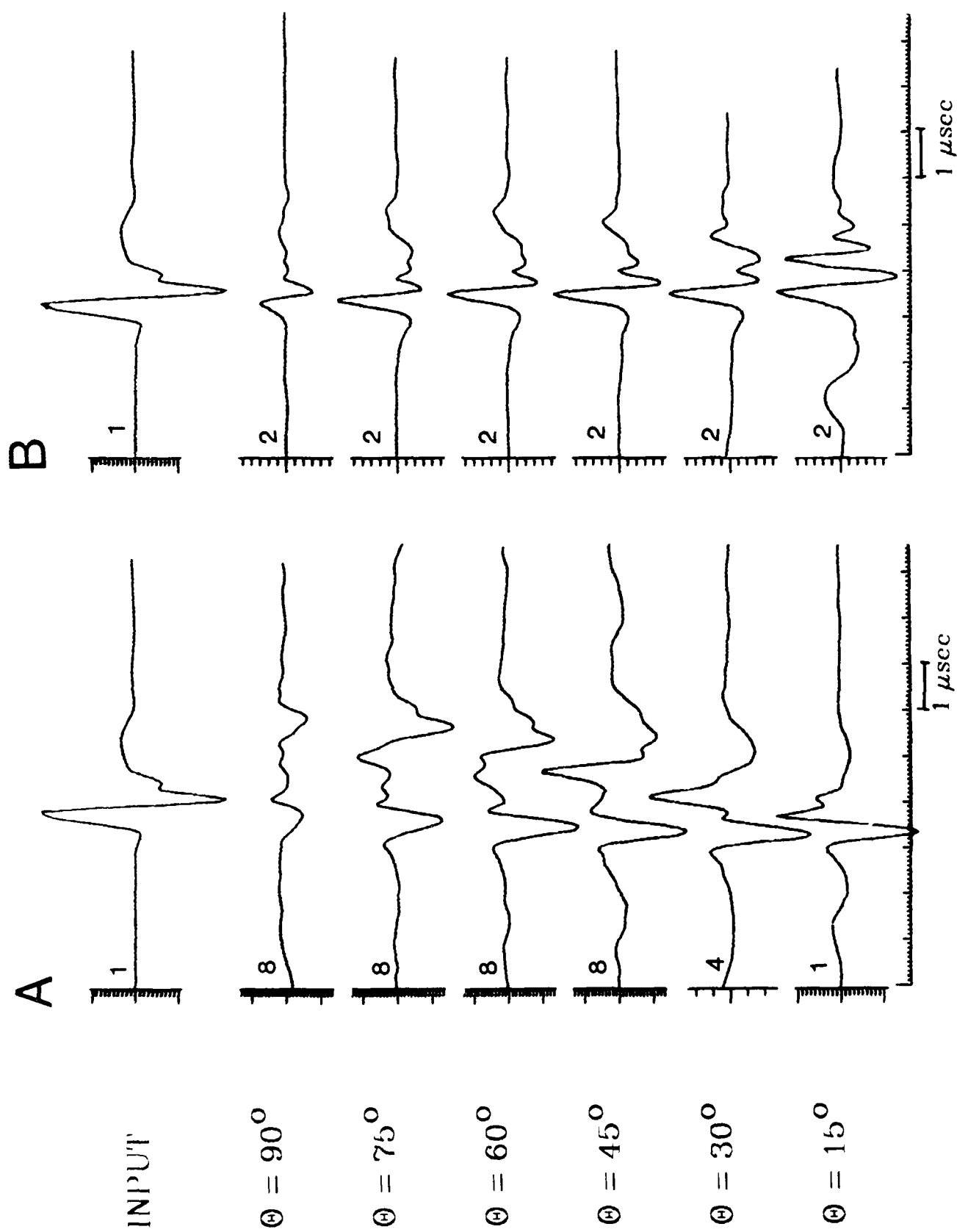


Figure 4

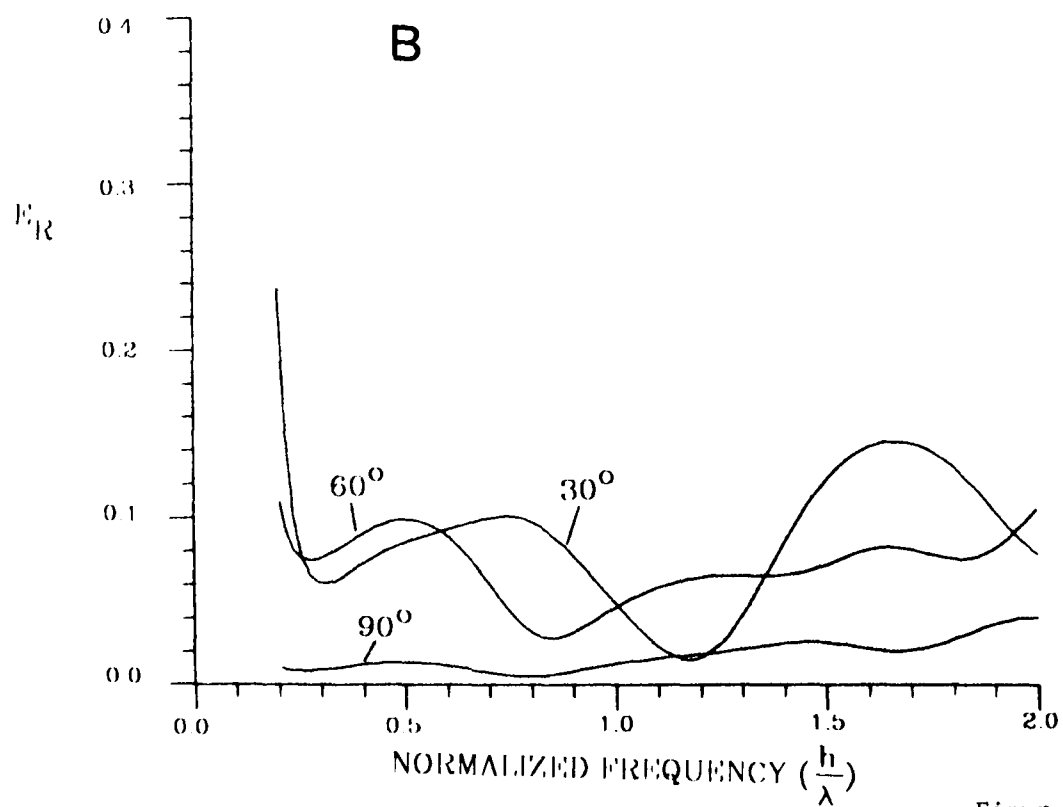
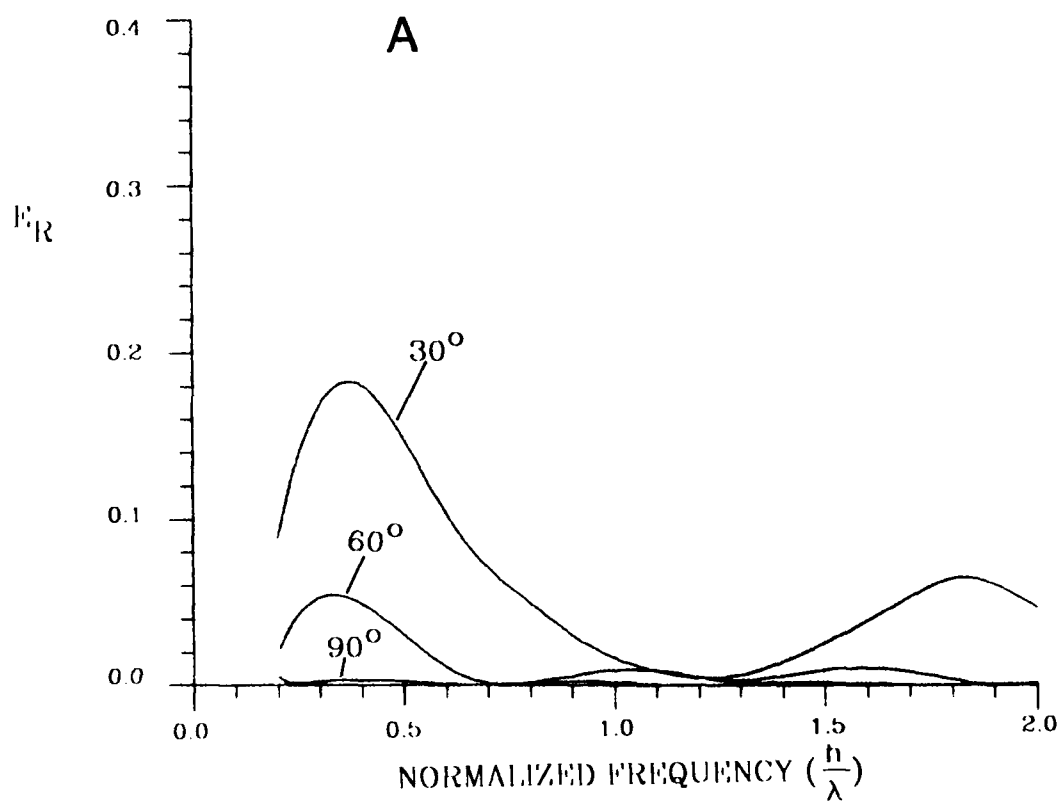


Figure 5

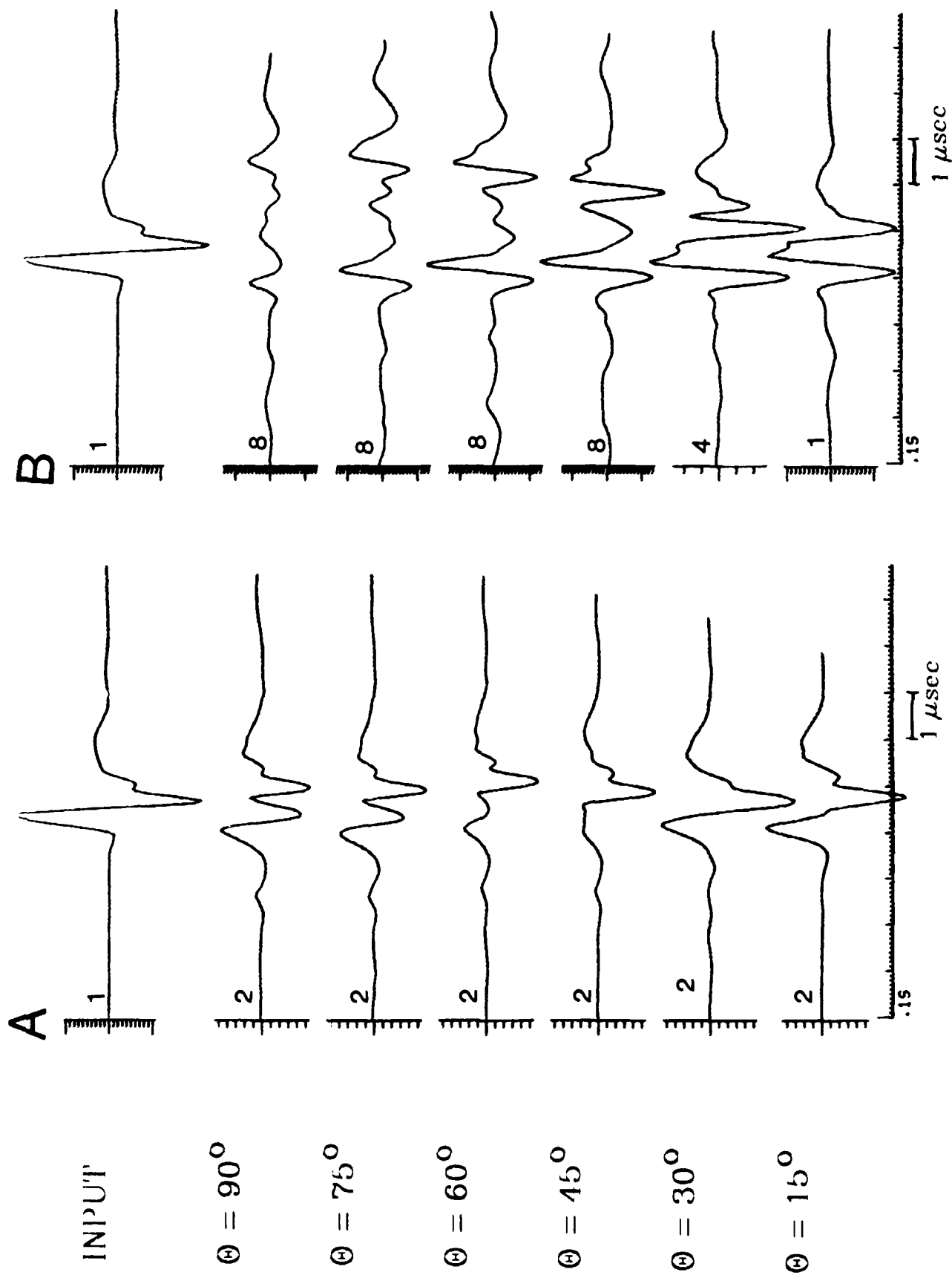


Figure 6

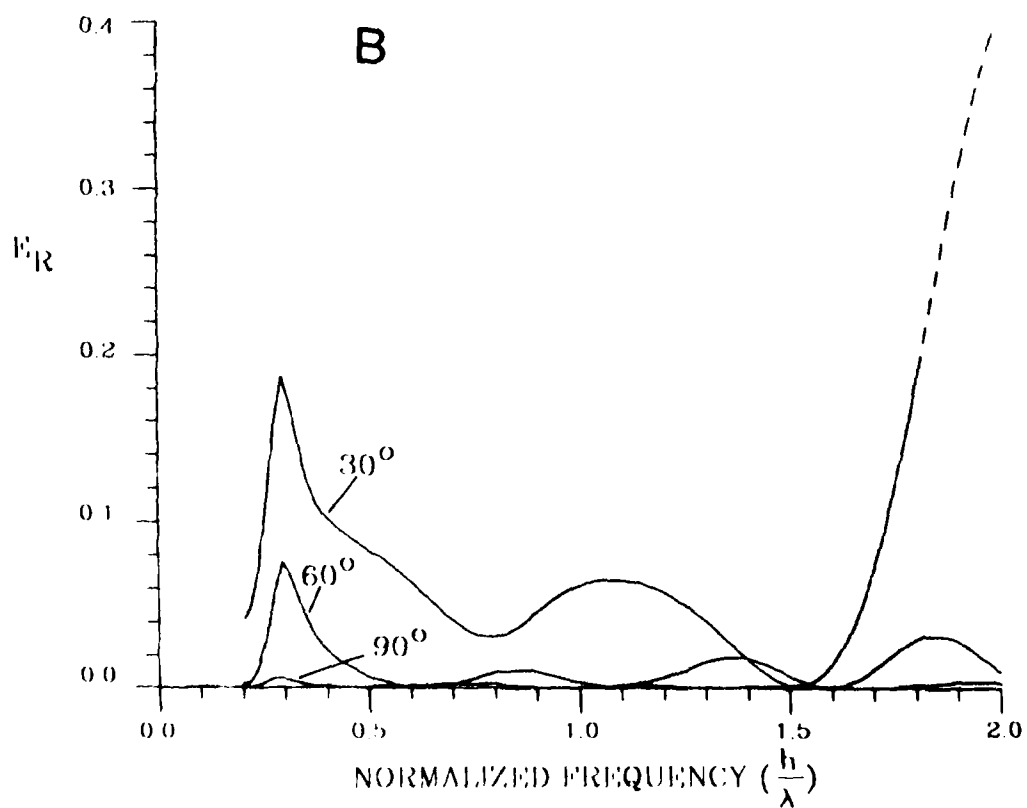
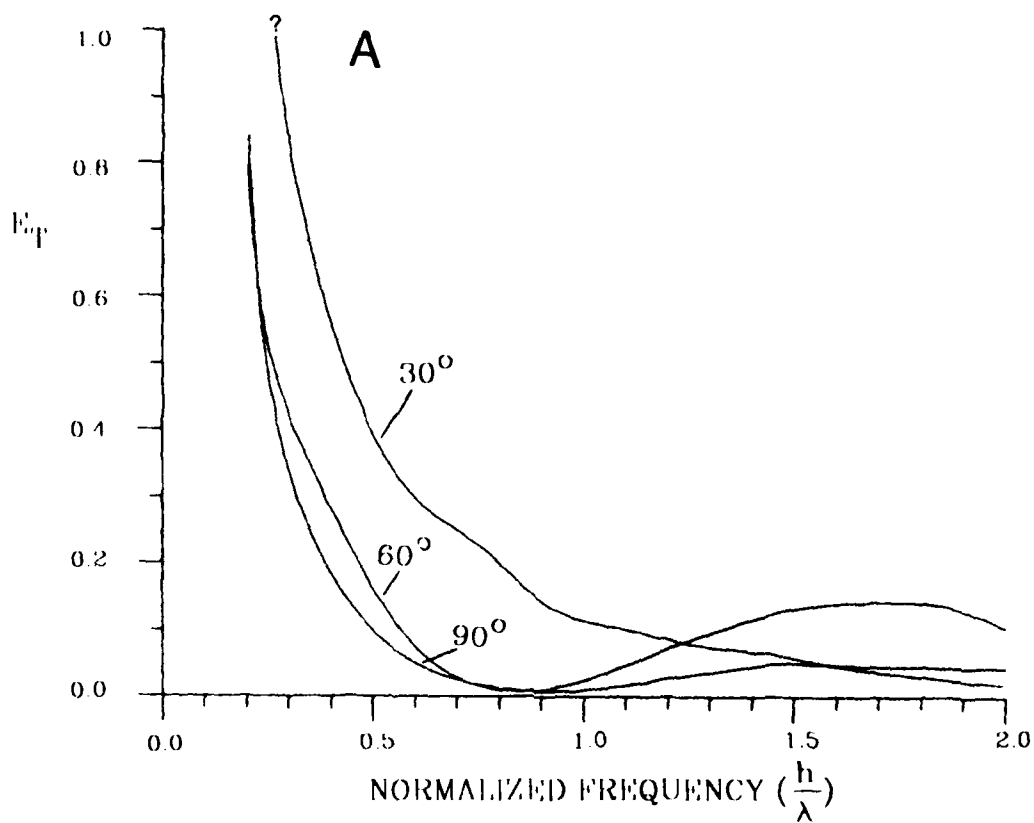


Figure 7

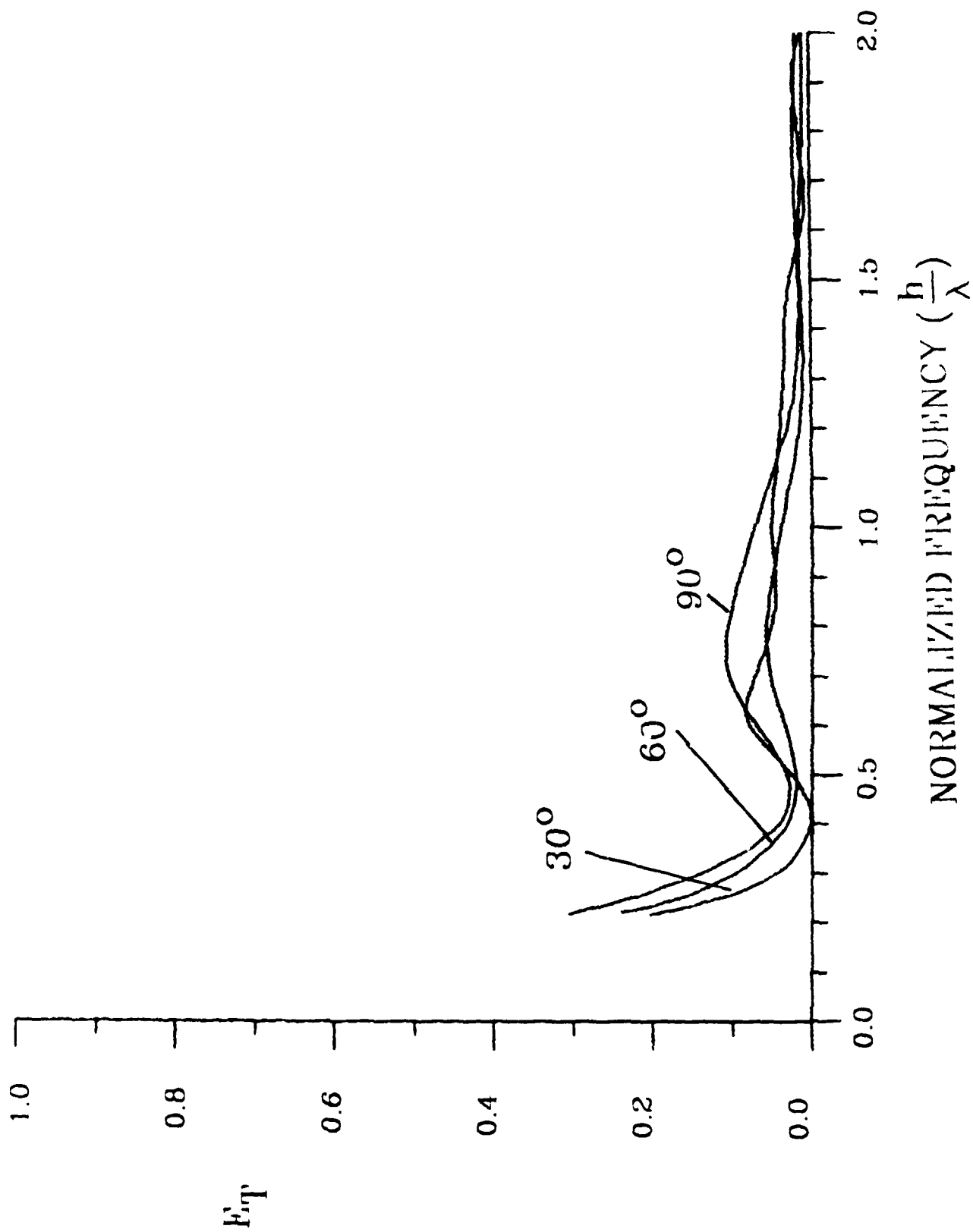


Figure 8

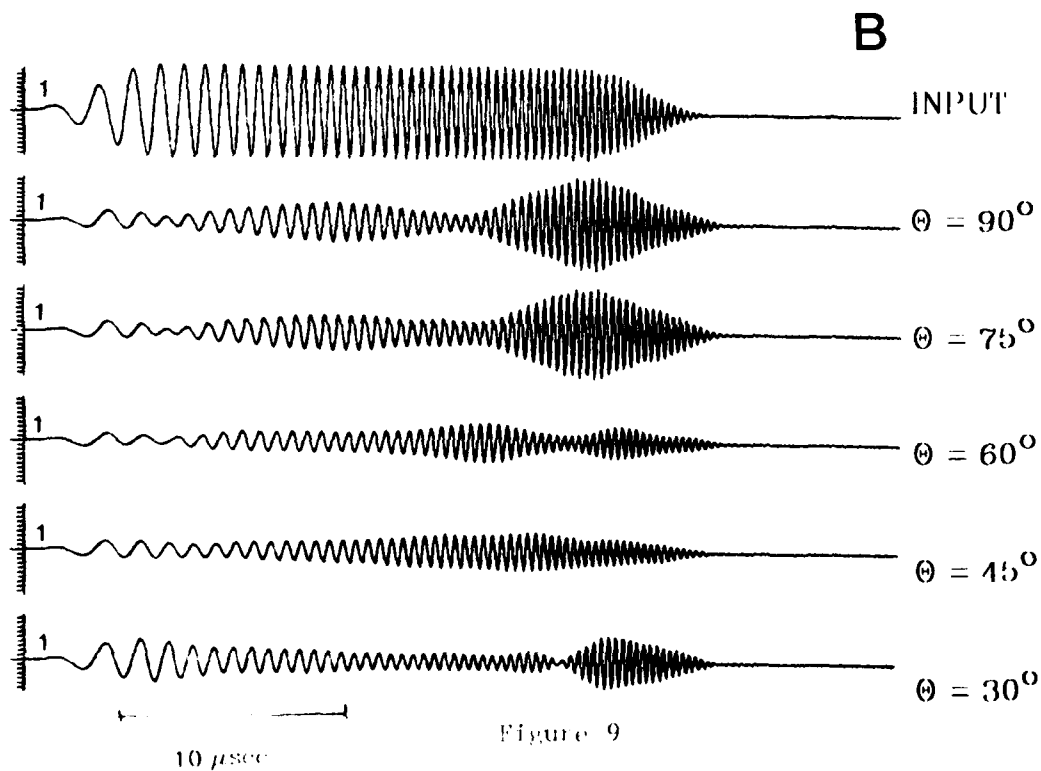
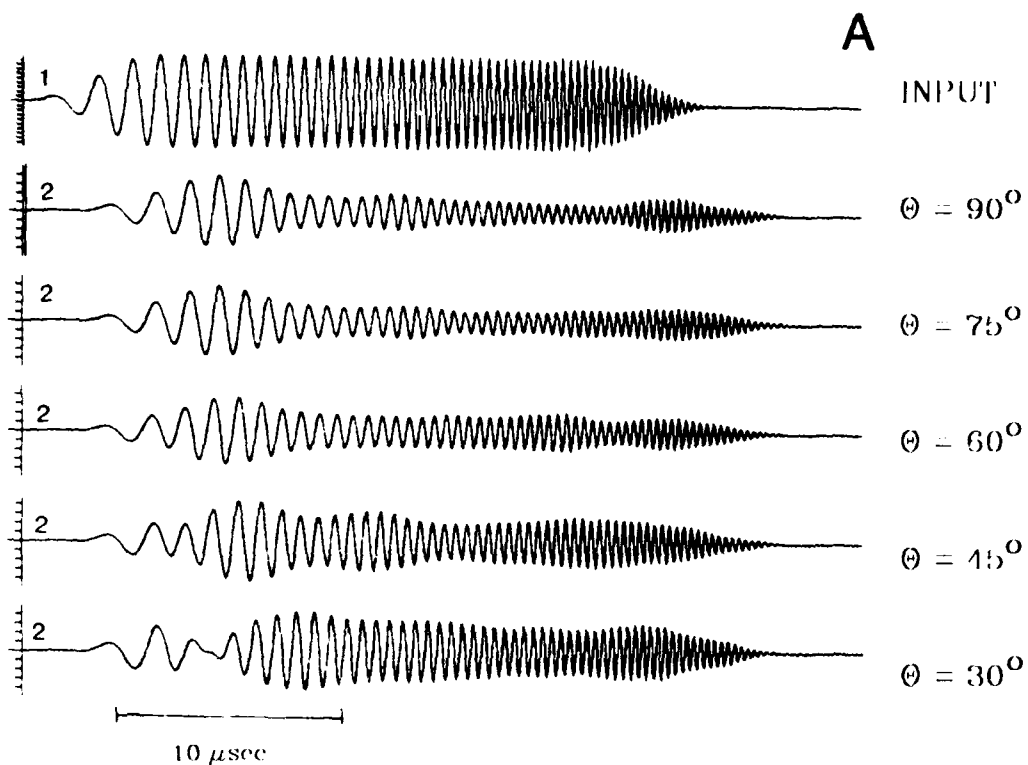


Figure 9

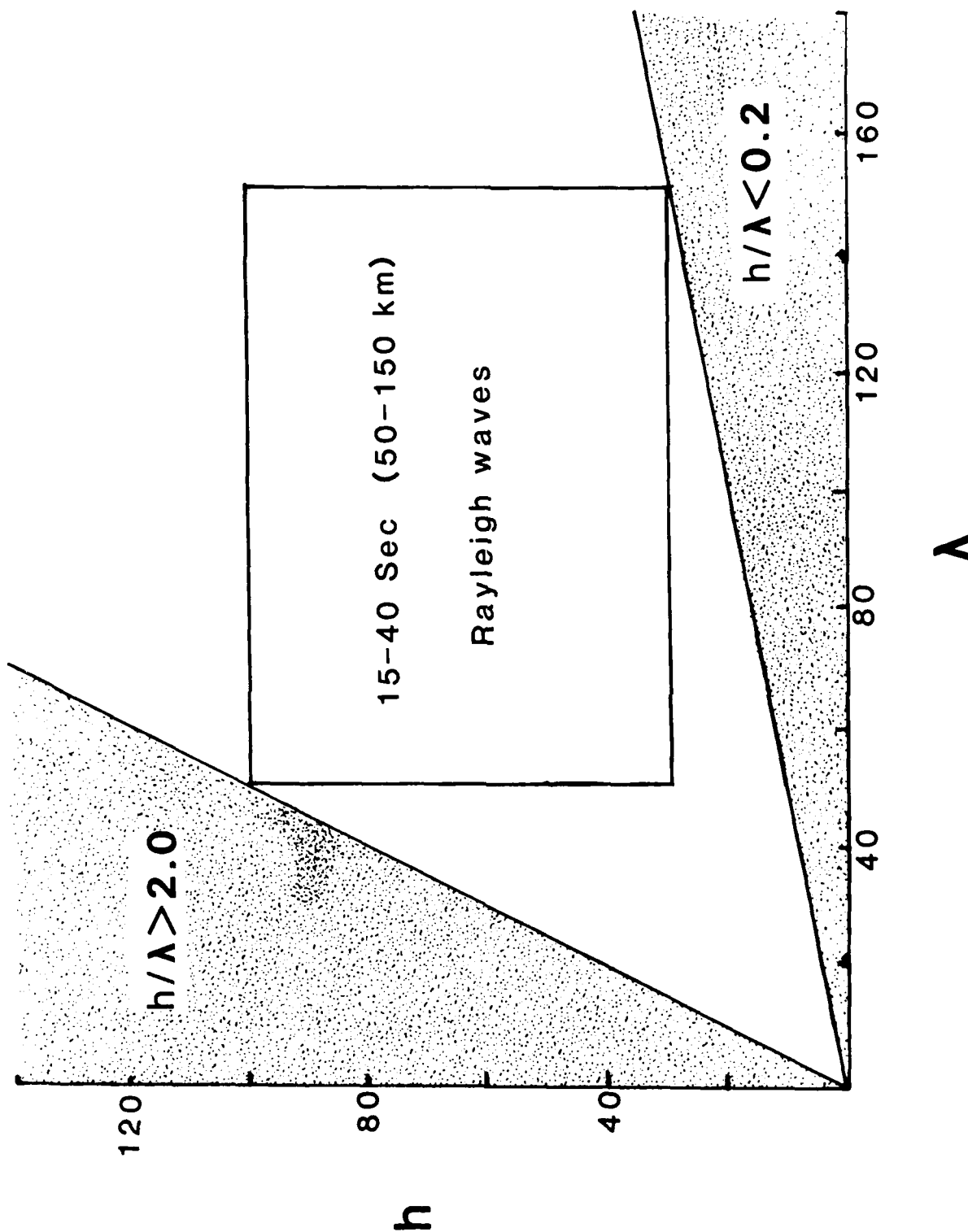


Figure 39

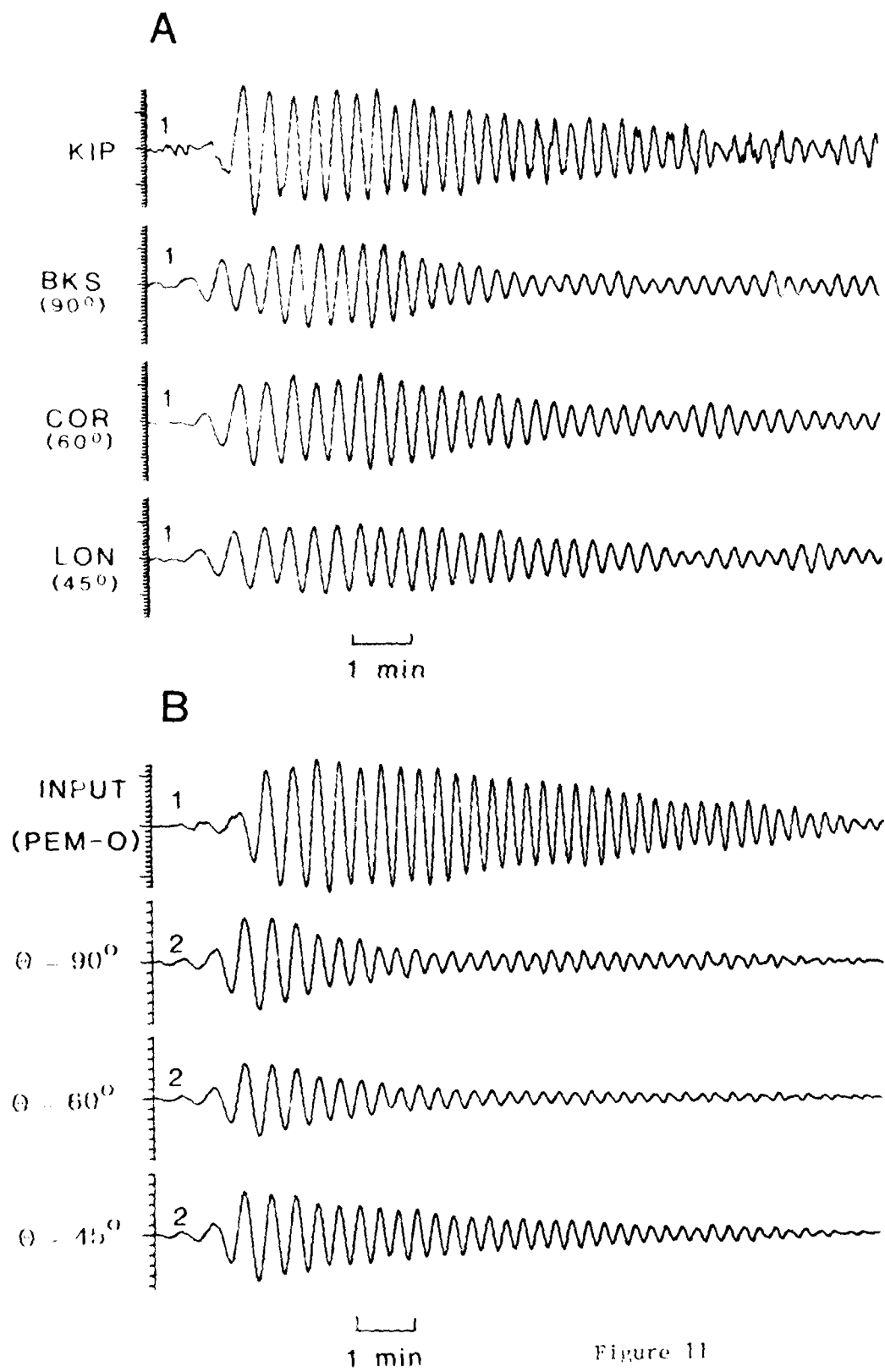


Figure 11

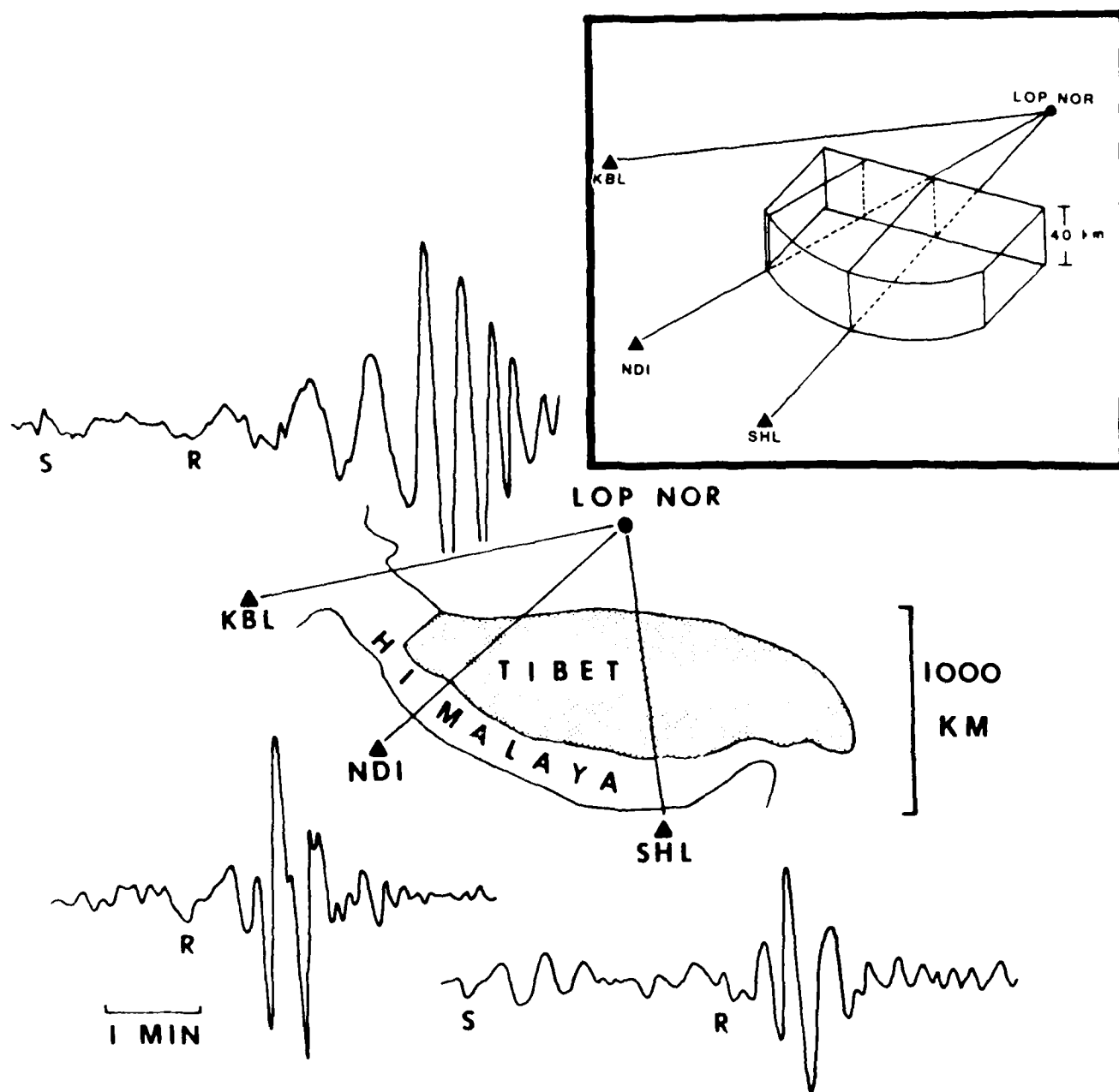


Figure 12

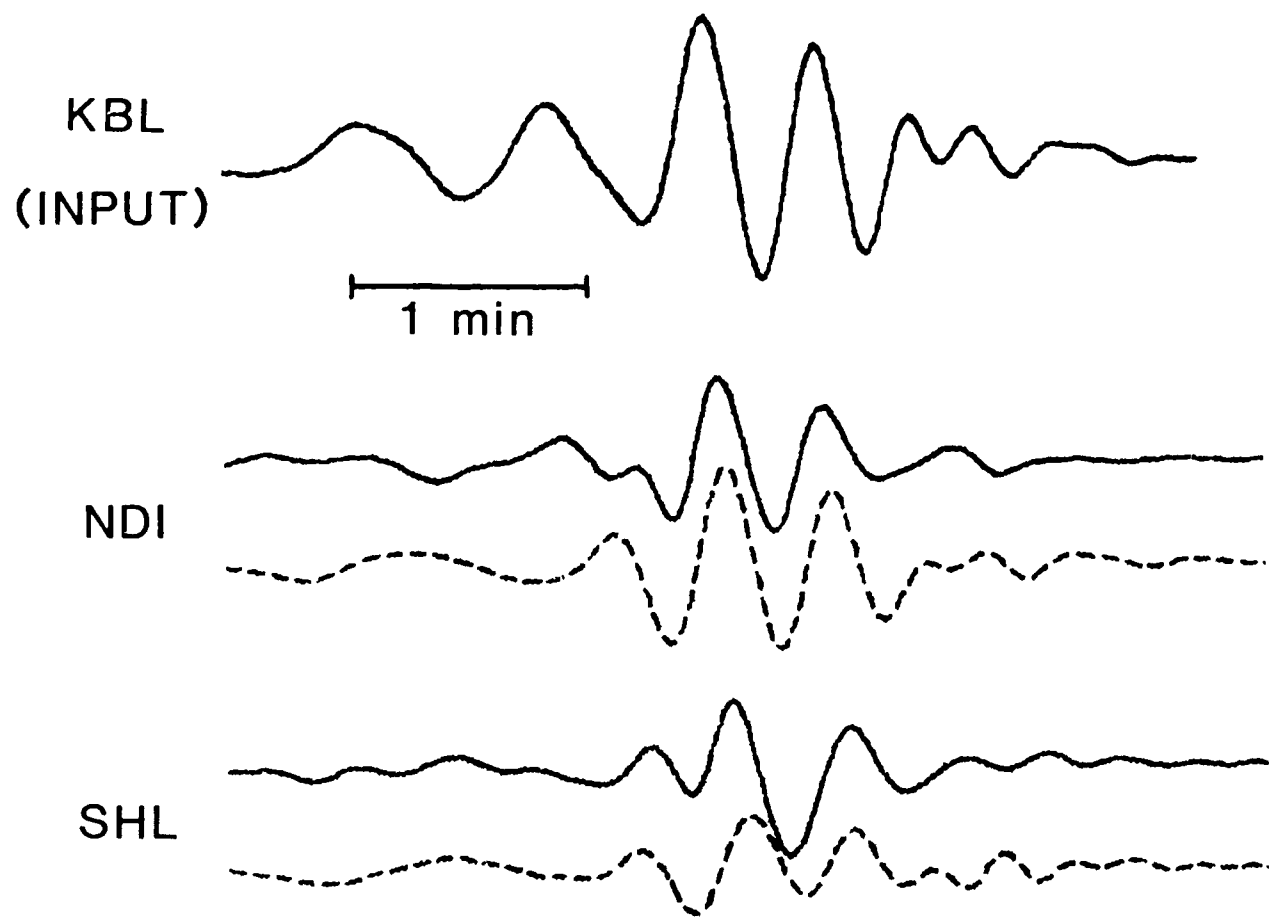


Figure 13

END

FILMED

7-85

DTIC